

# ELECTRON MICROSCOPE RADIOAUTOGRAPHY AS A QUANTITATIVE TOOL IN ENZYME CYTOCHEMISTRY

## II. The Distribution of DFP-Reactive Sites at Motor Endplates of A Vertebrate Twitch Muscle

M. M. SALPETER

From the Department of Applied Physics and Section of Neurobiology and Behavior, Division of Biology, Cornell University, Ithaca, New York

### ABSTRACT

The distribution of diisopropylfluorophosphate (DFP)-sensitive enzyme sites at the neuromuscular junction was determined quantitatively by electron microscope radioautography after incubation of muscle fragments in DFP- $^3\text{H}$ . Most of the sensitive sites were located in the subneural apparatus at a concentration of 90,000 sites per  $\mu^3$  of cleft tissue or 12,000 sites per  $\mu^2$  of postjunctional membrane surface area. A considerable concentration is also present in the telogial cap. It has previously been demonstrated (Rogers et al., 1966) that one-third of the DFP-sensitive sites at the endplate can be reactivated by pyridine-2-aldoxime methiodide (2-PAM)—a compound which selectively reactivates phosphorylated acetylcholinesterase. In the present study, it was found that this ratio of 1:2 holds also on a fine-structural level. Muscle mast cells were found to have a heavy concentration of bound DFP.

The use of radioactive diisopropylfluorophosphate (DFP) to label tissue acetylcholinesterase (AChE) was first suggested by Ostrowsky and Barnard (1961). Rogers et al. (1966, 1969) improved and standardized these procedures (see also review by Barnard and Rogers, 1967). DFP, one of the organophosphate nerve gases, is a potent inhibitor of cholinesterases as well as of other carboxylic acid esterases, and acts by phosphorylating the enzyme sites (for review, see Dixon and Webb, 1964). When muscle fragments are incubated in radioactive DFP, the distribution of tissue esterases is reflected by the distribution of tissue radioactivity and can be studied quantitatively.

A similar procedure was used by Waser and Reller (1965).

Rogers et al. (1966, 1969) manipulated the system in order to label acetylcholinesterase (AChE) separately from the other DFP-reactive sites. They accomplished this by combining the use of radioactive DFP with that of nonradioactive DFP and with the oxime, pyridine-2-aldoxime methiodide (2-PAM), which selectively reactivates phosphorylated AChE under their experimental conditions (Wilson, Ginsburg, and Quan, 1958; Wilson, 1966). Reversible enzyme inhibitors (such as eserine) were also used to protect different sites from radioactive DFP. They concluded that ap-

proximately one-third of the DFP-sensitive sites at the endplate was AChE and that the remaining two-thirds were 2-PAM-resistant sites. Less than 10% of the total DFP-phosphorylated sites represented serum cholinesterase (ChE).

In an earlier paper, I analyzed the distribution in the endplate of the 2-PAM-reactivated sites on a fine-structural level (Salpeter, 1967). In the present study, a similar analysis is performed for the DFP-phosphorylated sites which are not easily reactivated by 2-PAM, and the distributions of the two are compared.

## MATERIALS AND METHODS

**LABELING OF TISSUE:** Mouse sternomastoid muscle was used. The tissue was labeled by the procedures standardized by Rogers and Barnard<sup>1</sup> (Rogers et al., 1966, 1969; Barnard and Rogers, 1967). Two different labeling regimes were employed. Regime 1 was designed to phosphorylate only AChE with DFP-<sup>3</sup>H. The procedure was as described in a previous publication (Salpeter, 1967). Small pieces of muscle were first fixed in glutaraldehyde (1.5% in 0.06 M phosphate buffer at pH 7.4) for 2 hr and then thoroughly rinsed in buffer. Glutaraldehyde fixation decreases the uptake of DFP at motor endplates by, at most, about 10% (Rogers et al., 1966). The muscle was then incubated in nonradioactive DFP ( $10^{-3}$  M in phosphate buffer pH 7.4) at room temperature for 20 min to phosphorylate all DFP-sensitive sites, and then washed several times in buffer for a total of 20 min. It was then incubated in 2-PAM ( $10^{-3}$  M) at room temperature for 40 min to reactivate the AChE, washed in cold buffer, and left in buffer overnight. Radioactive DFP was then introduced into the reactivated sites by incubating the muscle in DFP-<sup>3</sup>H ( $10^{-4}$  M at 2.56 or 4.32 c/mmole) for 30 min at room temperature. The tissue was finally rinsed first in buffer and then in nonradioactive DFP (10 min in  $10^{-3}$  M followed by 1 hr in  $10^{-4}$  M), and then overnight in buffer. This sequence (nonradioactive DFP-2-PAM-DFP-<sup>3</sup>H) introduces radioactivity only into DFP-sensitive sites that had been reactivated by 2-PAM. The final washes in nonradioactive DFP and buffer minimize nonspecific radioactivity loosely bound to the tissue. The muscle was then postfixed in OsO<sub>4</sub>, stained in uranyl nitrate, and embedded in Epon 812.

Regime 2 was designed to phosphorylate only 2-

<sup>1</sup> The labeled muscle material used was kindly prepared by Dr. A. W. Rogers at the Molecular Enzymology Unit, Department of Biochemical Pharmacology, State University of New York at Buffalo in a program of A. W. Rogers and E. A. Barnard supported by NIH GM 11754.

PAM-insensitive sites with DFP-<sup>3</sup>H. The tissue was fixed in glutaraldehyde as in regime 1 and then incubated in DFP-<sup>3</sup>H ( $10^{-4}$  M at 4.32 c/mmole) for 30 min so as to introduce radioactivity into all the reactive sites. A washing sequence in nonradioactive DFP and buffer followed as in the last step of regime 1. The muscle was then incubated in 2-PAM ( $10^{-3}$  M) at room temperature for 40 min to reactivate the AChE and washed in buffer overnight. This sequence (DFP-<sup>3</sup>H-2-PAM) thus leaves radioactivity only in those DFP-sensitive sites not reactivated by 2-PAM. The specificity and reliability of these procedures have been demonstrated by Rogers et al. (1966, 1969) and Barnard and Rogers (1967). Since DFP phosphorylates enzyme sites stoichiometrically in a 1 to 1 ratio, one can equate the number of bound DFP molecules with active enzyme sites. DFP combines also with nonenzymatic sites, but at a considerably slower rate.

## Radioautography

**SPECIMEN PREPARATION:** Specimens were prepared for EM radioautography by the procedure of Salpeter and Bachmann (1964, 1965; see also Salpeter, 1966). Conditions for quantitative measurements were strictly applied (Bachmann and Salpeter, 1965, 1967). Sections having silver and pale gold interference colors were placed on collodion-coated slides, and their thickness was then measured with an interferometer (Reichert Instruments, W. Caldwell, N. J.). We found that in each case pale gold sections measure on the average 1,000 Å and silver sections about 800 Å, with all measurements deviating from the mean by less than 10%. This confirms the findings of Peachey (1958) and Bachmann and Sitte (1958). The sections were then stained with 1% uranyl acetate for 3 hr and vacuum coated with carbon. The gold sections were coated with a monolayer of Ilford L4 (judged by purple interference color) while the silver sections were coated with a monolayer of Kodak NTE (judged by pale gold interference color). The correlation between emulsion thickness and interference color is given in previous publications (Salpeter and Bachmann, 1964, 1966). After 15–27 wk of exposure, the Ilford L4-coated slides were developed with Microdol X (Eastman Kodak Co., Rochester, N. Y.) for 3 min at 24°C and the Kodak NTE slides were developed with the gold latensification–Elon ascorbic acid method, also at 24°C. The specimens were stripped off the slides, picked up on copper electron microscope grids, and examined with an RCA EMU3 electron microscope.

**ANALYSIS OF EM RADIOAUTOGRAPHS:** Random pictures of muscle were first taken for obtaining a value for the extent of muscle background (i.e. developed grains per unit area of muscle). Grain densities associated with the different regions of the

endplate were then obtained. Three regions were considered: the nerve endbulb, the junctional fold zone, and the teloglia cap—a region of connective tissue and Schwann cell cytoplasm overlying the nerve bulb (Couteaux, 1958). Grids were scanned completely, and all endplates were photographed, whether or not there were developed grains associated with them. All radioautographs were magnified to 30,000. The location of each developed grain was defined by its center which was determined as follows: a small plastic mask on which were drawn differently sized circles concentric around a common perforated center was laid over the grain, and the grain was fitted into the smallest circle which fully circumscribed it. The center was then punched with a dissecting needle onto the print.

So as to provide an easy means for tabulating data as grain density (i.e., grains per unit area), the area occupied by the different regions of the endplate was determined as follows: a board containing a grid of equally spaced nails was fitted exactly over each radioautograph, and the nails were punched through the print. The resultant lattice of points, which are completely unbiased (random) with respect to any tissue components, were then tabulated in the same manner as were the grains. Grain density was expressed either as grains per point or, since the average number of points per square micron of radioautograph was easily calculated and the thickness of the sections known, as grains per  $\mu^2$ . Under the conditions of this study, the number of developed grains was found to increase linearly with exposure time. The number of developed grains was, therefore, convertible to the number of radioactive decays in the tissue per unit time of exposure (using sensitivity values previously established—Bachmann and Salpeter, 1967). Finally, since the specific activity of the DFP- $^3\text{H}$  was known (giving the number of decays per mole of DFP per unit of time), and since one DFP molecule phosphorylates one active enzyme site, an easy calculation further converted grain density to molecules of DFP or phosphorylated enzyme per cubic micron of tissue.

One cannot, however, convert grain density to radioactive decays in the tissue without considering the scattered grains. Because of the spread of radiation from a radioactive source, developed grains do not lie immediately above a source in the tissue, but distribute themselves in some statistical manner around the source. Therefore, the developed grains immediately over a structure represent only a fraction of the developed grains which are due to radioactive decays within that structure. The extent to which this would effect the accuracy of any conversion from grain density to radioactive decays depends on, among other things, the size of the radioactive area. The relative number of total grains that lie outside a radioactive structure decreases as the size of the struc-

ture increases. (Salpeter et al., 1969 have shown that, under the average conditions of resolution used in this study,<sup>2</sup> less than 30% of the developed grains would lie outside a radioactive structure that is approximately 1  $\mu$  in radius, whereas more than 75% would lie outside this structure were it 0.1  $\mu$  in radius.) Thus for small radioactive structures, the radiation spread must be considered before a conversion from grain density to radioactive decays is valid.

It was, therefore, first essential to define the radioactive structures as accurately as possible. This was done by plotting grain density distributions around different components of the endplate and determining the peaks and general shapes of these distributions. In the postjunctional region, grain density distributions were obtained in relation to both axonal and postjunctional membranes. This was done as follows: the perpendicular distance from every developed grain center and from every lattice point was measured first to the axonal membrane and then to the postjunctional membrane. A grain distribution histogram (total grains per unit distance from the membrane) was plotted separately for these two membranes. The distance had a negative sign if the grain or point lay on the axonal side of the particular membrane and a positive sign if it lay on the muscle side of the membrane. Similar histograms were also plotted for the lattice points. When the number of grains in each histogram column was divided by the number of points in the same histogram column, an accurate correction for area was made and the grain distributions were converted to a grain density distribution.

All distances were measured in units of "HD"—a measure of resolution.<sup>2</sup> When plotted in distance units of HD, grain density distributions have a universal shape. This allows data from different specimens to be combined (Salpeter et al., 1969).

## RESULTS

A typical section through an endplate is illustrated in Fig. 1, and typical radioautographs in Figs. 2 and 3. The nerve endbulb sits in a trough at the

<sup>2</sup> In a recent study, Salpeter et al. (1969) have measured resolution experimentally for a variety of EM radioautographic specimens differing in section thickness and emulsion and developer combinations. They found that for each specimen there is a value for "half-distance" (HD) which is characteristic of its resolution. HD is the distance from a line source in such a specimen within which 50% of the developed grains would fall. The HD values for the two specimen conditions used in this study are 1200 A (for the silver section, Kodak NTE emulsion, Elon ascorbic acid development) and 1600 A (for the pale gold section, Ilford L4 emulsion, and Microdol X development).

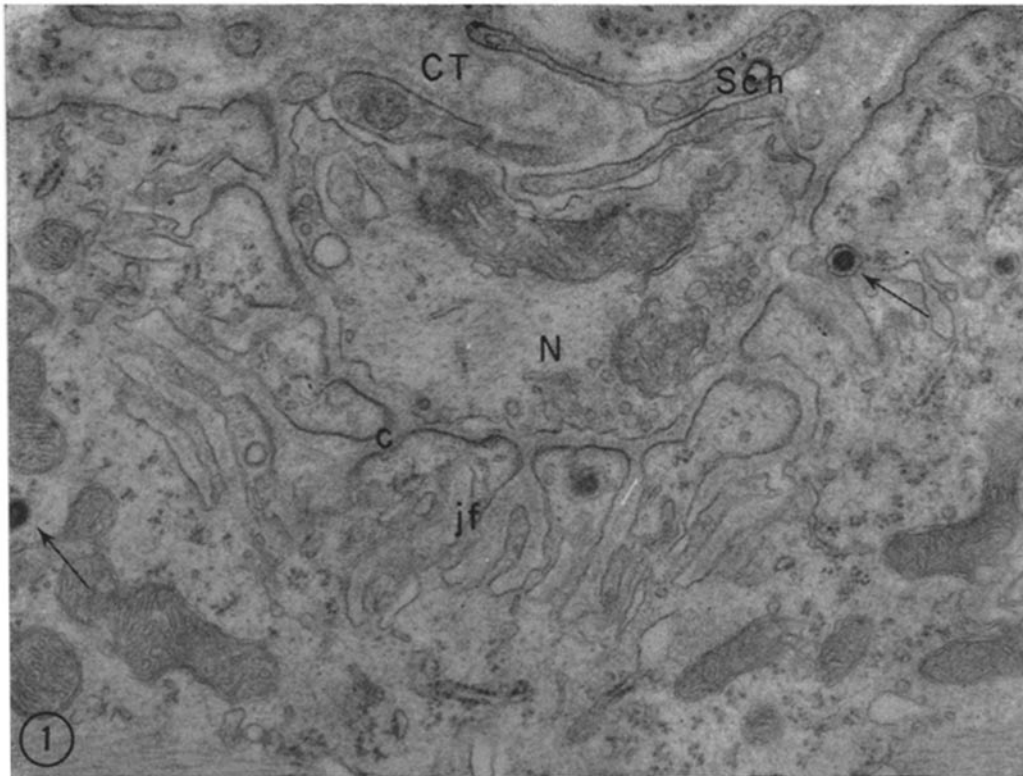


FIGURE 1 Typical electron micrograph of a motor endplate in this material. Nerve terminal (*N*) sits in trough formed by the invagination and infolding of postjunctional muscle membrane (*jf*). The teloglia cap consists of tongues of Schwann cytoplasm (*Sch*) and connective tissue (*CT*). The Schwann cell does not make a close seal over the nerve (see also Fig. 2). The clefts (*c*) separate axon from junctional folds. Dense granules (arrows) are characteristically seen on the muscle side of the endplate. In radioautographs of this material, such granules were never selectively associated with developed grains.  $\times 30,000$ .

surface of the muscle fiber. The plasma membrane of the muscle is thrown into characteristic junctional folds. Dense-core vesicles are seen among these folds. Overlying the nerve bulb is the teloglia cap consisting of loosely interwoven Schwann cytoplasm and bands of connective tissue. The Schwann cytoplasm does not seal the nerve from the extracellular space—separations of several thousand Angstroms between nerve endbulb and Schwann cell are common, as are large gaps in the Schwann cell cover. In this study the teloglia cap was arbitrarily defined as the connective tissue and Schwann cells within a zone 4HD (6400 Å) wide overlying the nerve endbulb.

#### *Location of Radioactivity*

In the first paper of this series (Salpeter, 1967), the relative radioactivity (representing labeled

AChE) between postjunctional region and teloglia cap was  $\sim 85 : 10$ . A similar distribution was seen in the present study with both labeling regimes. Preliminary counts indicate that in the teloglia cap there was a peak grain density on the Schwann plasma membrane, with less over the connective tissue, and possibly only scattered grains over Schwann cytoplasm. The total number of grains in the cap was too low, however, (66 grains) to make a statistically valid comparison of radioactivity in connective tissue versus Schwann cytoplasm. The cap was, therefore, treated as a unit.

In the postjunctional region, however, the grain yield was much higher (848 grains) and a more detailed analysis was possible. Figs. 4 and 5 are grain density distributions with respect to the axonal plasma membrane, obtained from radio-

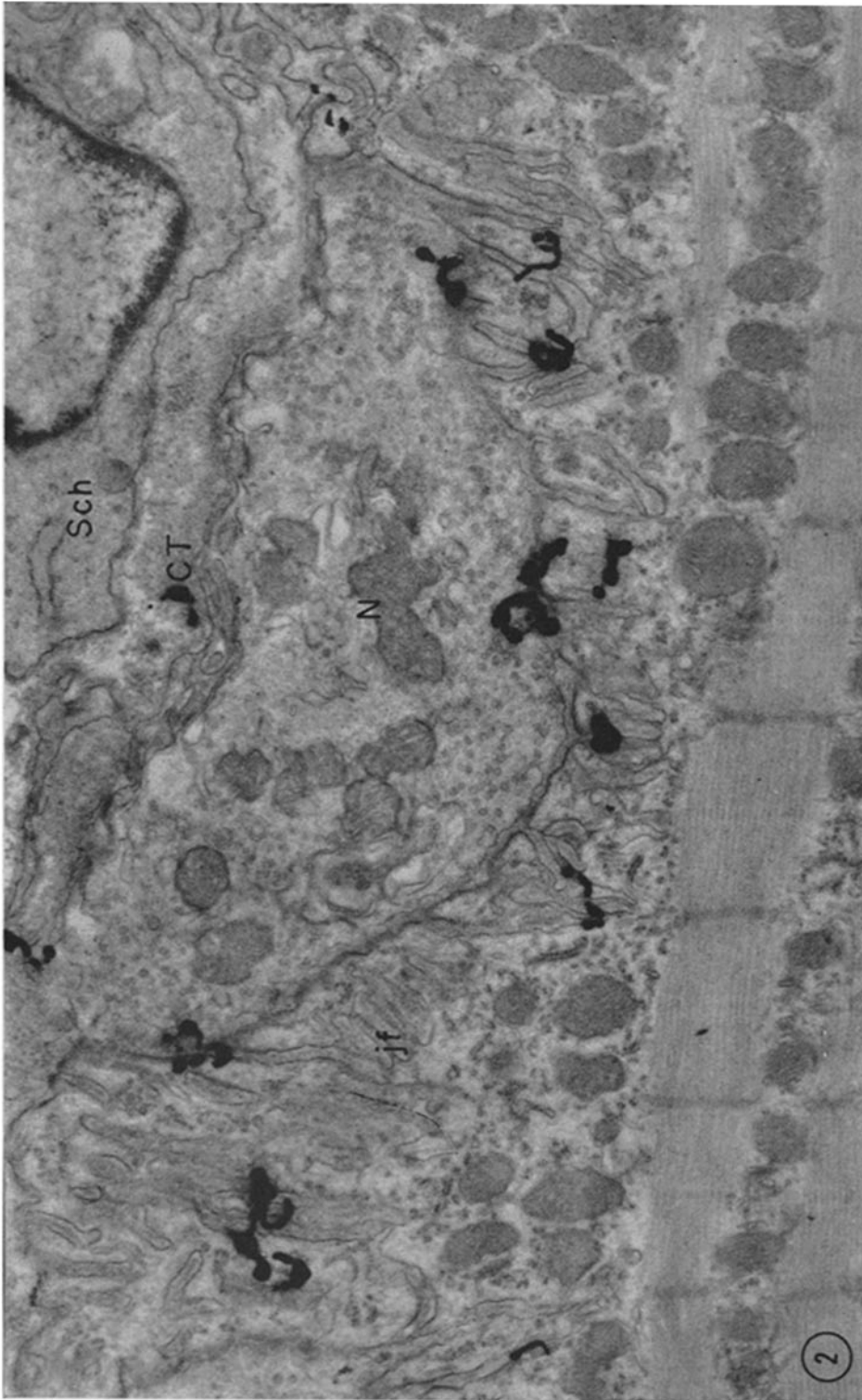


FIGURE 2 Radioautograph of DPP-<sup>3</sup>H at endplate after the incubation sequence DPP-<sup>3</sup>H-2-PAM. Pale gold section coated with Ilford L4, Microdol X developed. Developed grain are seen over junctional folds (*jf*) and telogial cap (*Sch* + *CT*), but not over nerve terminal (*N*). X 20,000.



FIGURE 3 Radioautograph of tissue treated as in Fig. 2. Silver section coated with Kodak NTE, gold latensification-Elon ascorbic acid developed. Note developed grains (arrows) mainly over junctional folds.  $\times 45,000$ .

autographs after the two DFP-labeling regimes. It is clear from these histograms that the bulk of the radioactivity after both labeling regimes lies to the muscle side of the axonal membrane in a band corresponding to the junctional fold zone.

When tabulated in relation to the postjunctional membrane, the location of the radioactivity becomes much better defined (illustrated in Figs. 6-8). There is a distinct peak of grain density over the postjunctional membrane after both labeling regimes. The theoretical distributions superimposed on the experimental histograms are from Salpeter et al. (1969). They represent the expected grain density distribution around a line source with a slight curvature equal to the typical curvature of the nerve endbulb. Since the junctional folds have a somewhat more complicated geometry than would be given by a straight line source, the theoretical curve is only an approximation. It fits the experimental distributions remarkably well, however. Owing to the limits set

by the resolution of the EM radioautographic technique, the data are compatible with either of two hypotheses: (1) that the radioactivity is associated with the junctional membranes, or (2) that it is associated with the postjunctional clefts (a band of  $\sim 700 \text{ \AA}$ ).

#### *Enzyme Concentrations*

Grain density was converted to density of bound DFP- $^3\text{H}$  molecules (i.e., active sites) in the tissue (Table I). Because of the greater stability of Ilford L4 with prolonged exposures (Bachmann and Salpeter, 1967), only radioautographs from tissue coated with Ilford L4 and developed with Microdol X were used for this conversion. Under the conditions of this experiment, one developed grain represented, on the average, 10 radioactive decays (sensitivity value from Bachmann and Salpeter, 1967). The specific activity of the DFP gave the relationship between radioactive decays and molecules of DFP and, thus, active sites.

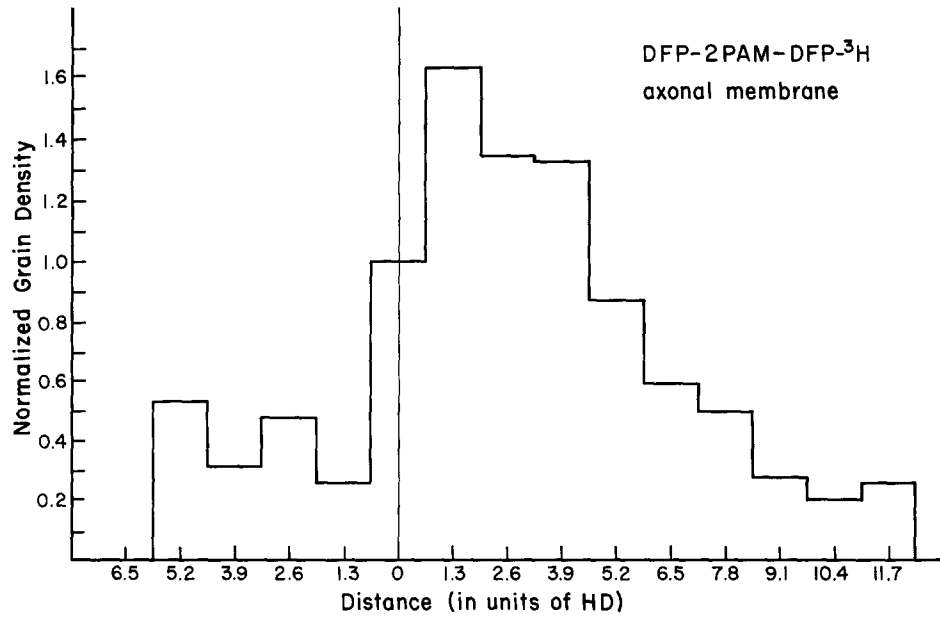


FIGURE 4 Grain density (i.e., grains/points) with distance either side of axonal membrane (axonal membrane at 0). Labeling sequence was DFP-2-PAM-DFP-<sup>3</sup>H, which introduces radioactivity selectively into 2-PAM-reactivated sites, i.e., AChE. On the left, the histogram goes into the nerve; on the right, into the muscle. Distance was measured in microns and then divided by the HD value characteristic for the given specimen. (Tabulating distance in units of HD allowed data from the two specimen conditions, i.e. Ilford L4 coated and Kodak NTE coated, to be combined [Salpeter et al. 1969].) Density was normalized to 1.0 at the origin. The grain density peaks over a broad zone which is coincident with the junctional folds. (Based on 272 grains.)

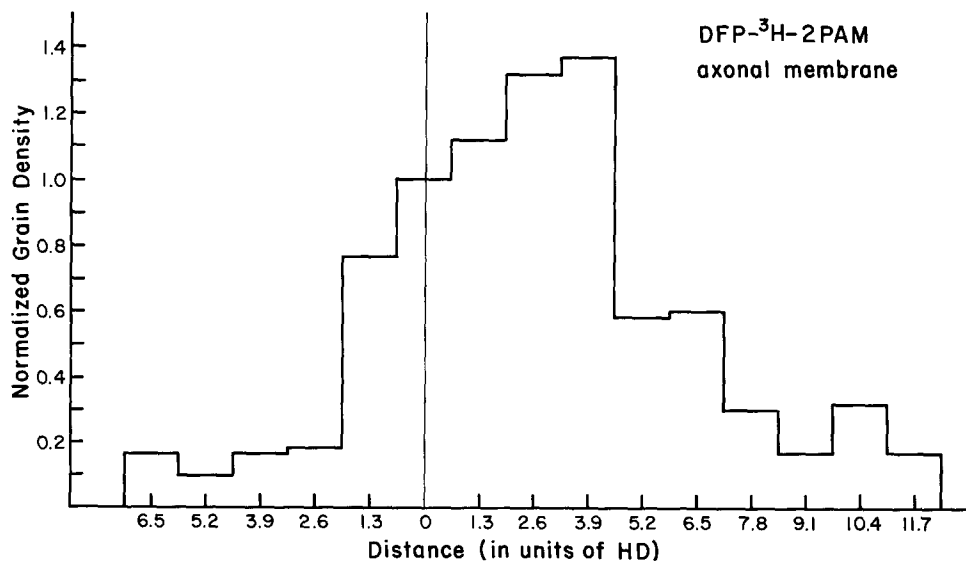


FIGURE 5 Histogram obtained as in Fig. 4, except for the labeling sequence DFP-<sup>3</sup>H-2-PAM, which introduces radioactivity selectively into 2-PAM-nonreactivated sites. The general distributions in Figs. 4 and 5 are similar. (Based on 437 grains.)

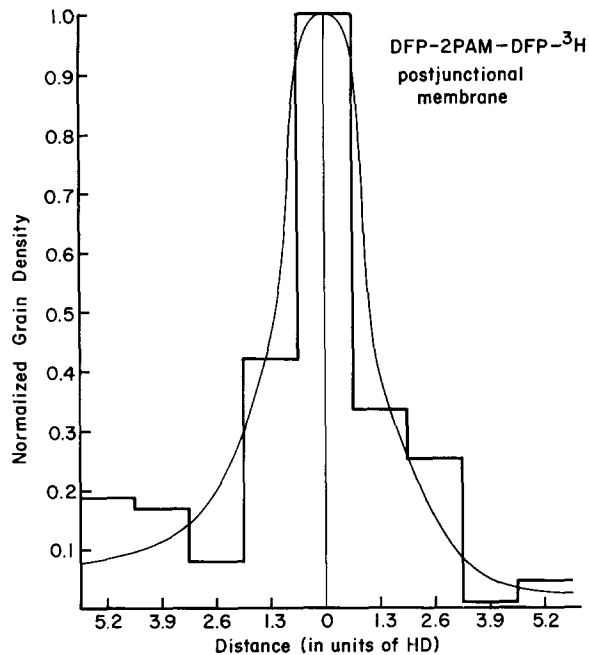


FIGURE 6 Histogram of grain density (grains/points) with distance either side of postjunctional membrane for the labeling sequence DFP-2PAM-DFP- $^3\text{H}$  (i.e., 2-PAM-reactivated sites). Left side of histogram goes towards the nerve, right side towards muscle. Distance was measured in units of HD as in Fig. 4, and the data from Ilford L4 and Kodak NTE specimen were combined. Grain density was normalized to 1.0 at origin. The smooth curve superimposed on the histogram represents the expected distribution, if the radioactivity was confined to a line (or thin band) following the postjunctional membrane. (A correction for the slight curvature given by the shape of the muscle trough produces the left-to-right asymmetry.) The theoretical distribution is from Salpeter et al. (1969). (Histogram is based on 307 grains.)

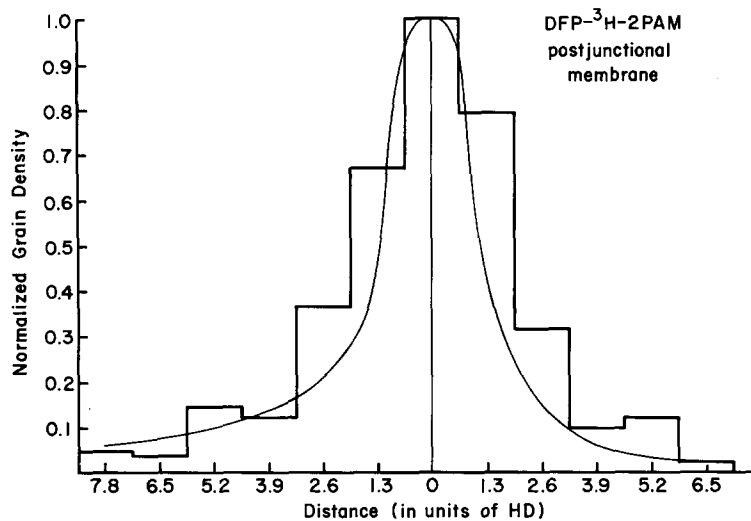


FIGURE 7 Histogram and superimposed curve obtained as for Fig. 6 except for 2-PAM-nonreactivated sites. (Based on 541 grains.)

In the postjunctional region, the grain density distributions (Figs. 6-8) indicated that the radioactivity was confined to a relatively narrow band and, as discussed above, there was, therefore, a need to make a correction for the spread of radiation. From the density histograms, the radioactivity in the postjunctional region could be related

either to the junctional membranes or to the  $\sim 700 \text{ \AA}$  cleft adjacent to them. Enzyme concentrations were calculated for both of these possibilities, in each case correcting for scattered developed grains. This correction was done by considering all the grains which fitted the expected density distribution (Figs. 6 and 7) as belonging

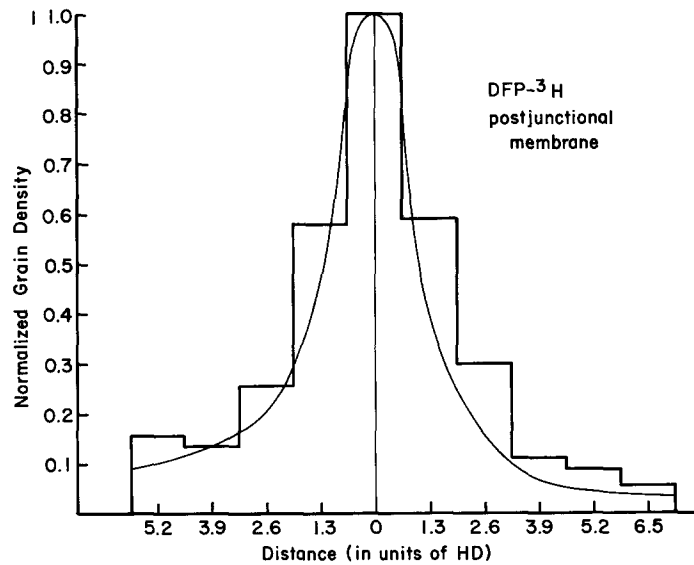


FIGURE 8 Grain density around postjunctional membrane for total DFP-sensitive sites obtained by adding data (grains and points) from both labeling sequences (DFP-<sup>3</sup>H-2-PAM and DFP-2-PAM-DFP-<sup>3</sup>H). (Based on 848 grains.)

to the radioactive region. The surface area of junctional membrane was obtained by measuring its length in all the radioautographs with a map measurer and multiplying this length by the thickness of the section. The volume of the cleft was obtained from the number of lattice points lying over cleft tissue in the radioautographs. Values for grains per  $\mu^2$  of surface membrane or  $\mu^3$  of cleft were then converted to enzyme concentrations.

Since no precise localization of radioactivity was accomplished for the telogial cap, the entire volume of the telogial cap was used for the density determination. The value given in Table I for the telogial cap thus represents a lower limit.

Rogers et al. (1966, 1969) have shown that in the endplate, as a whole, the two sites (2-PAM nonreactivated, and 2-PAM reactivated) appear quantitatively in the ratio of about 2 to 1. From Table I, it can be seen that the two sites appear in the same ratio also on a fine-structural level within the limit of resolution attained in this study.

#### *Labeling Other than at Endplate*

**MAST CELL:** An immediate and striking observation when looking at radioautographs of muscle fragments which had been incubated in

DFP-<sup>3</sup>H is the massive labeling over the cytoplasm of mast cells lying between the muscle fibers. (The sensitivity of mast cells to DFP has earlier been reported by Langunoff and Benditt, 1963.) Rogers et al. (1966) have suggested that, with unstained tissue and light microscope radioautography, images of labeled muscle mast cells could have been mistaken for endplates in the study by Ostrowski and Barnard (1961; see also Barnard and Ostrowski, 1964). Fig. 9 shows a fragment of a mast cell labeled by the regime DFP-<sup>3</sup>H-2-PAM. Darzynkiewicz and Barnard (1967) have shown that the DFP-sensitive sites in the mast cell are not reactivated by 2-PAM. This thus represents all the DFP-sensitive sites. The radioautographic exposure time is equal to that of the endplate in Fig. 2. With this exposure, the emulsion over the mast cell is clearly saturated and no quantitation was possible. Yet with similar material exposed for only 2 wk, a rough tabulation gave a value of  $1.9 \times 10^5$  DFP molecules bound per cubic micron of mast cell cytoplasm. The grains appear concentrated in the granules rather than distributed uniformly throughout the cytoplasm (see also Budd et al., 1967). Thus, the value per cubic micron of granule would be even higher (almost twice that value) since the granules occupy just over half the volume of the cytoplasm.

In a recent publication, Darzynkiewicz and Barnard (1967) give a value of  $6 \times 10^3$  molecules of DFP bound per peritoneal mast cell which has a diameter  $16.1 \mu$ . A rough tabulation indicates

TABLE I  
Concentration of DFP Molecules Bound at Endplate

Tissue component	Density $\times 10^3$		Ratio
	DFP- <sup>3</sup> H-2-PAM	DFP-2-PAM-DFP- <sup>3</sup> H	
Muscle	$0.54/\mu^3$	$0.53/\mu^3$	1.0
Subneural zone*			
Clefts	$62.0/\mu^3$	$28.0/\mu^3$	2.2
Postjunctional membrane	$8.2/\mu^2$	$3.8/\mu^2$	2.2
Nerve terminal‡	—	—	—
Telogliial cap§	$5.6/\mu^3$	$2.3/\mu^3$	2.4

Concentration of DFP molecules bound at the endplate was determined from grain density values after appropriate corrections were made for scattered radiation. (A correction was also made for a possible 10% loss of active sites due to glutaraldehyde fixation.) Total DFP bound per tissue component is given by the sum of columns 1 and 2. \* In the subneural zone, enzyme densities were calculated both per  $\mu^3$  of cleft tissue and per  $\mu^2$  of postjunctional membrane surface.

‡ Grain density distributions (Figs. 4-8) suggest that any developed grains over the nerve terminal are due to radiation spread from its radioactive surroundings.

§ The volume of the telogliial cap was determined by the total number of grid points which fell over Schwann cytoplasm and collagen fibrils within 4 HD (6,400 Å) from the nerve endbulb. Since a preliminary analysis suggests that the radioactivity is concentrated within a smaller volume, the density value given here represents a lower limit, but is probably correct to within a factor of two.

that in these cells approximately  $\frac{1}{6}$  of the cell volume is nucleus. The cells that Darzynkiewicz and Barnard studied thus had a cytoplasmic volume of  $1.8 \times 10^3 \mu^3$  and a density of bound DFP molecules equal to  $3.3 \times 10^5$  per  $\mu^3$  of cytoplasm. This value agrees, within a factor of two, with the value calculated here per  $\mu^3$  of muscle mast cell cytoplasm (i.e.,  $1.9 \times 10^5$ ).

MUSCLE: There is a certain amount of grain density over the muscle, which we have called muscle background. It is about two to three times above off-section, or true, background, and is equivalent to about 500 DFP molecules bound per  $\mu^3$  of muscle tissue (Table I). This quantity is approximately the same after both labeling regimes (DFP-<sup>3</sup>H-2-PAM and DFP-2-PAM-DFP-<sup>3</sup>H). (See also Salpeter, 1967.)

There is some evidence for the localization of esterases in muscle (Barnett and Palade, 1959; and Miledi, 1964). Preliminary histograms of grain density distributions within the muscle show no concentration over either the M or the Z bands. However, there is a tendency to have a slightly higher concentration near the muscle membrane. Rogers et al. (1966, 1969) suggest that much of the muscle activity represents low levels of residual adsorption of DFP rather than phosphorylated enzyme sites, although the latter possibility cannot be excluded. It appears, however, that whatever muscle esterases are present, their concentration is too low to be detected above the general background of adsorbed radioactivity, and must, therefore, be considerably less than 500 sites/ $\mu^3$ .

## DISCUSSION

DFP-sensitive sites at the endplate were determined quantitatively by electron microscope radioautography. Most of these sites (~80%)

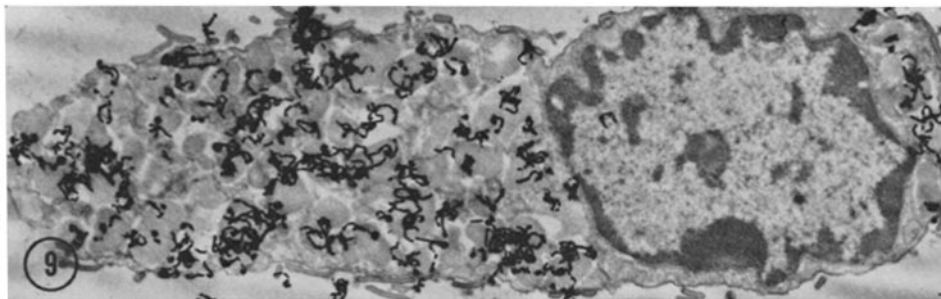


FIGURE 9 Mast cell between muscle fibers after labeling sequence DFP-<sup>3</sup>H-2-PAM. Radioautographic conditions as for endplate in Fig. 2.  $\times 7,700$ .

are within the subneural apparatus at a concentration of 90,000 sites per  $\mu^3$  of cleft tissue or 12,000 sites per  $\mu^2$  of postjunctional membrane. A significant concentration is also present in the teloglia cap (at least  $\sim 7,900$  sites per  $\mu^3$ ).

Rogers et al. (1966, 1969), using DFP- $^{32}\text{P}$  and light microscope radioautography, demonstrated that only about 30–40% of the DFP-sensitive sites at the endplate can be reactivated by 2-PAM (or are sensitive to eserine). They, therefore, conclude that only this one-third represents true AChE. The present study has shown that the 2 to 1 ratio for the 2-PAM-nonreactive and 2-PAM-reactive sites exists in the subneural apparatus also on the fine-structural level (Table I) and thus that the general distribution of these two DFP-sensitive sites is indistinguishable within the resolution limits set by the EM radioautographic technique (see also Fig. 8).

It is not yet clear what the 2-PAM-nonreactivated sites represent. Waser and Reller (1965) claim that all the DFP-reactive sites at the endplate are AChE. Yet Barnard and Rogers (1967) argue that the conditions of reactivation in their procedures exclude the possibility that ageing prevented the full reactivation of the phosphorylated AChE. Furthermore, Wiscowski and Barnard (1967) have shown that under conditions similar to those of this experiment only the DFP-phosphorylated enzyme sites which are reactivated by 2-PAM are essential for neuromuscular transmission. This is consistent with other data which indicate that 2-PAM can produce complete recovery of neuromuscular transmission after DFP poisoning (Wills et al., 1957; Namba and Heraki, 1968). The evidence thus suggests that the 2-PAM-insensitive sites are not directly necessary for neuromuscular transmission.

The 2-PAM-nonreactive sites may represent nonspecific or ali-esterases which are known to be sensitive to phosphorylation by DFP (see Dixon and Webb, 1964, for review). Yet this would contradict the available histochemical studies which find little evidence for the presence of eserine-insensitive esterases at the endplate (Denz, 1953; Zacks, 1964; Koelle and Gromadzki, 1966; Davis and Koelle, 1967). The histochemical literature is, however, not yet definitive, since there is still some disagreement on the relative concentrations of the different esterases at the motor endplate. Eranko and Teravainen (1967 *a, b*) and Teravainen (1967), for instance, do find some

eserine resistant or ali-esterases at normal, as well as at regenerating motor endplates. However, even in these studies, the nonspecific esterases appear to represent a smaller component than do the cholinesterases. The various histochemical results and the DFP data still have to be reconciled in determining the nature of the 2-PAM-nonreactive sites. The similarity in distribution of the two types of DFP-sensitive sites suggests the possibility that they are anatomically and (or) functionally linked. This suggestion is strengthened by the fact that in a completely different system, the rat megakaryocyte, there exists a similar two to one ratio between DFP-sensitive sites which are 2-PAM-resistant and those which are 2-PAM-sensitive (Darzynkiewicz et al., 1966).

The exact localization of esterases at the endplate is also still an open question. Light microscope histochemical studies had early designated the subneural apparatus as the primary site of esterase activity at the endplate (see review by Couteaux 1955, 1958). This is confirmed by the distribution of radioactivity in the present study. One hopes that finer localization will come from EM histochemistry which potentially has a much higher resolution than does EM radioautography. Unfortunately, however, problems of diffusion of reaction product have prevented, in several studies with EM histochemistry, the utilization of this higher resolution and the reaching of an agreement on whether the enzymes are located only on the membranes (Davis and Koelle, 1967; Bergman et al., 1967) or in the clefts as well (Barnett, 1962; Zacks and Bloomberg, 1961; Lehrer and Ornstein, 1959; Csillik, 1965). Recent studies have even suggested a postjunctional cytoplasmic localization for AChE (Teravainen, 1967). Until agreement is reached, it is not clear which of the values for enzyme concentration given in Table I provides the most meaningful biological information.

The number of developed grains found over the nerve was small. The data are compatible with a hypothesis that all the developed grains over the nerve could be due to the spread of radiation from its radioactive surroundings (see histograms in Figs. 4–8). Hoskin et al. (1966) have claimed that there is a DFPase present in squid nerve. If a DFP-hydrolyzing enzyme is also present in mouse nerve and if it remains active after glutaraldehyde fixation, it could explain the relative absence of bound radioactivity in the nerve. Yet the absence

of radioactivity is consistent with most of the histochemical studies which similarly do not get a reaction product deposited inside the nerve bulb.

A question frequently raised is whether or not there are any esterases on the axonal membrane. Many histochemical studies suggest that there are (e.g. Davis and Koelle, 1967; Barnett, 1962). Although EM radioautography cannot resolve radioactivity on the axonal membrane from that on the adjacent postjunctional membrane, the data in Figs. 4 and 5 do provide some quantitative information. The grain scatter seen in these figures is roughly what one would expect if the radioactivity was distributed in a band over the junctional fold region with an edge on or near the axonal membrane. There is no significant increase in grain density in the histogram column which contains both postjunctional membrane and axonal membrane (i.e., at the origin Figs. 4 and 5).

#### BIBLIOGRAPHY

- BACHMANN, L., and M. M. SALPETER. 1965. Autoradiography with the electron microscope. A quantitative evaluation. *Lab. Invest.* **14**:1041.
- BACHMANN, L., and M. M. SALPETER. 1967. Absolute sensitivity of electron microscope radioautography. *J. Cell Biol.* **33**:299.
- BACHMANN, L., and P. SITTE. 1958. Dickenbestimmung nach Tolansky an Ultradunnschnitten. *J. Microsc.* **13**:289.
- BARNARD, E. A., and K. OSTROWSKI. 1964. Autoradiographic methods in enzyme cytochemistry. II. Studies on some properties of acetylcholinesterase in its sites at the motor endplate. *Exp. Cell Res.* **36**:28.
- BARNARD, E. A., and A. W. ROGERS. 1967. Determination of the number, distribution, and some *in situ* properties of cholinesterase molecules in the motor endplate, using labeled inhibitor methods. *Ann. N. Y. Acad. Sci.* **144**:584.
- BARNETT, R. J. 1962. The fine structural localization of acetylcholinesterase at the myoneural junction. *J. Cell Biol.* **12**:247.
- BARNETT, R. J., and G. E. PALADE. 1959. Enzymatic activity in the M band. *J. Biophys. Biochem. Cytol.* **6**:163.
- BERGMAN, R. A., H. UENO, Y. MOUZONO, J. S. HANKER, and A. M. SELIGMAN. 1967. Ultrastructural demonstration of acetylcholinesterase activity of motor endplates via osmiophilic diazothioesters. *Histochemie.* **11**:1.
- BUDD, G. C., Z. DARZYNKIEWICZ, and E. A. BARNARD. 1967. Intracellular localization of specific proteases in rat mast cells. *Nature.* **213**:1202.
- COUTEAUX, R. 1955. Localization of cholinesterases at neuromuscular junctions. *Int. Rev. Cytol.* **5**:335.
- COUTEAUX, R. 1958. Morphological and cytochemical observations on the post-synaptic membrane at motor endplates and ganglionic synapses. *Exp. Cell Res. Suppl.* **5**:294.
- CSILLIK, B. 1965. Functional structure of the post-synaptic membrane in the myoneural junction. Akademiai Kiadó, Publishing House of the Hungarian Academy of Science, Budapest.
- DARZYNKIEWICZ, Z., and E. A. BARNARD. 1967. Specific proteases of the rat mast cell. *Nature.* **213**:1198.
- DARZYNKIEWICZ, Z., A. W. ROGERS, and E. A. BARNARD. 1966. Quantitative analysis of the esterases in the rat megakaryocytes by a radioisotope cytochemical technique. *J. Histochem. Cytochem.* **14**:379.
- DAVIS, R., and G. B. KOELLE. 1967. Electron microscope localization of acetylcholinesterase and non-specific cholinesterase at the neuromuscular junction by the gold-thiocholine and gold-thiolacetic acid methods. *J. Cell Biol.* **34**:157.
- DENZ, F. A. 1953. On the histochemistry of the myoneural junction. *Brit. J. Exp. Pathol.* **34**:329.
- DIXON, M., and E. WEBB. 1964. Enzymes. Academic Press Inc., New York.
- ERANKO, O., and H. TERAVAINEN. 1967 *a*. Cholinesterases and eserine resistant carboxylic esterases in degenerating and regenerating motor endplates of the rat. *J. Neurochem.* **14**:947.
- ERANKO, O., and H. TERAVAINEN. 1967 *b*. Distribution of esterases in the myoneural junction of the

- striated muscle of the rat. *J. Histochem. Cytochem.* **15**:399.
- HOSKIN, F. C. G., P. ROSENBERG, and M. BRZIN. 1966. Re-examination of the effect of DFP on electrical and cholinesterase activity of squid giant axon. *Proc. Nat. Acad. Sci.* **55**:1231.
- KOELLE, G. B., and C. G. GROMADZKI. 1966. Comparison of the gold-thiocholine and gold-thioacetic acid methods for the histochemical localization of acetylcholinesterase and cholinesterases. *J. Histochem. Cytochem.* **14**:443.
- LAGUNOFF, D., and E. P. BENDITT. 1963. Proteolytic enzymes of mast cells. *Ann. N. Y. Acad. Sci.* **103**:185.
- LEHRER, G. M., and L. ORNSTEIN. 1959. A diazo coupling method for electron microscopic localization of cholinesterase. *J. Biophys. Biochem. Cytol.* **6**:399.
- MILEDI, R. 1964. Electron-microscopical localization of products from histochemical reactions used to detect cholinesterase in muscle. *Nature.* **204**:293.
- NAMBA, T. and K. HERAKI. 1968. PAM (pyridine-2-aldoxime methiodide) therapy for alkylphosphate poisoning. *J. Amer. Med. Ass.* **166**:1834.
- OSTROWSKI, K., and E. A. BARNARD. 1961. Application of isotopically labelled specific inhibitors as a method in enzyme cytochemistry. *Exp. Cell Res.* **25**:465.
- PEACHEY, L. D. 1958. Thin sections. I. A study of section thickness and physical distortion produced during microtomy. *J. Biophys. Biochem. Cytol.* **4**:233.
- ROGERS, A. W., Z. DARZYNKIEWICZ, E. A. BARNARD, and M. M. SALPETER. 1966. Number and location of acetylcholinesterase molecules at motor endplates of the mouse. *Nature.* **210**:1003.
- ROGERS, A. W., Z. DARZYNKIEWICZ, K. OSTROWSKI, M. M. SALPETER, and E. A. BARNARD. 1969. Quantitative studies on enzymes in structures in striated muscles by labeled inhibitor methods. I. The number of acetylcholinesterase molecules and of other DFP-reactive sites at motor endplates measured by radioautography. *J. Cell Biol.* **41**:665.
- SALPETER, M. M. 1966. General area of autoradiography at the electron microscope level. *In* Methods in Cell Physiology. D. Prescott, editor. Academic Press Inc., New York. **2**:229.
- SALPETER, M. M. 1967. Electron microscope radioautography as a quantitative tool in enzyme cytochemistry. I. The distribution of acetylcholinesterase at motor endplates of a vertebrate twitch muscle. *J. Cell Biol.* **32**:379.
- SALPETER, M. M., and L. BACHMANN. 1964. Autoradiography with the electron microscope. A procedure for improving resolution, sensitivity and contrast. *J. Cell Biol.* **22**:469.
- SALPETER, M. M., and L. BACHMANN. 1965. Assessment of technical steps in electron microscope autoradiography. *In* Use of Radioautography in Investigation of Protein Synthesis. Symposium of the International Society for Cell Biology. C. P. Leblond and C. A. Warren, editors. Academic Press Inc., New York.
- SALPETER, M. M., L. BACHMANN, and E. E. SALPETER. 1969. Resolution in electron microscope radioautography. *J. Cell Biol.* **41**:1.
- TERAVAINEN, H. 1967. Electron microscopic localization of cholinesterases in the rat myoneural junction. *Histochemie.* **10**:266.
- WASER, P. G., and J. RELLER. 1965. Bestimmung der zahl aktiver Zentren der Acetylcholinesterase in motorischen Endplatten. *Experientia.* **21**:402.
- WIESCOWSKI, J., and E. A. BARNARD. 1967. Correlation between the number of AChE molecules inactivated at a neuromuscular junction and its response to electrical impulses. *J. Cell Biol.* **35**:143A. (Abstr.)
- WILLS, J. H., A. M. KUNKEL, R. V. BROWN, and G. E. GROBLEWSKI. 1957. Pyridine-2-aldoxime methiodide and poisoning by anticholinesterases. *Science.* **125**:743.
- WILSON, I. B. 1966. The inhibition and reactivation of acetylcholinesterase. *Ann. N. Y. Acad. Sci.* **135**:177.
- WILSON, I. B., S. GINSBURG, and C. QUAN. 1958. MOLECULAR complementarity as basis for reactivation of alkyl phosphate-inhibited enzyme. *Arch. Biochem. Biophys.* **77**:286.
- ZACKS, S. I. 1964. The Motor Endplate. W. B. Saunders Co., Philadelphia.
- ZACKS, S. I., and J. M. BLUMBERG. 1961. The histological localization of acetylcholinesterase in the finestructure of neuromuscular junctions of mouse and human intercostal muscle. *J. Histochem. Cytochem.* **9**:317.